33RD CONGRESS
OF THE INTERNATIONAL COUNCIL
OF THE AERONAUTICAL SCIENCES
STOCKHOLM, SWEDEN, 4-9 SEPTEMBER, 2022

ICAS 2022 SWEDEN

DESIGN OF AN INNOVATIVE WING TIP FOR AEROELASTIC CONTROL: FROM SCRATCH TO FLIGHT TEST

Francesco Toffol[1], Federico Fonte[1*], Sergio Ricci[1]

[1]Politecnico di Milano, Department of Aerospace Science and Technology, via la Masa 34, 20156, Milano, Italy

[*]Currently Rotor Dynamics, Leonardo Helicopter Division, 21017, Cascina Costa, Italy

Abstract

This paper resumes the activities done in the framework of the Clean Sky 2 AIRGREEN2 project, where an Innovative Wing Tip (IWT) device was designed, built, and tested. The IWT is equipped with an actively controlled movable surface for the active load reduction of the gust and maneuver load alleviation (MLA/GLA). The design involved several disciplines like aerodynamics, structure, actuation, sensing and control. Intermediate wind tunnel models and ground demonstrator provided experimental evidence of the reliability of the concept. The aim of this paper is to illustrate the process that led to the manufacturing of the IWT, which will be tested in flight by the end of 2023.

Keywords: Wing tip device, load control, gust loads alleviation

1. The AIRGREEN2 project

The Clean Sky 2 program (2015-2022) aimed to develop and consolidate new technologies to reduce the environmental footprint of new generation aircraft and rotorcraft. There were several platforms and among them the AIRGREEN2 [1] project was focused on new generation regional aircraft aiming at low emissions and noise. The reference aircraft was a turboprop that can accommodate up to 90 pax, named TP90, originally designed by Leonardo Velivoli and illustrated in Figure 1.

Figure 1 - TP90 illustration

In this framework, a consortium made of several industrial partners, research institutes and universities, developed an innovative morphing wing equipped with innovative devices to improve the efficiency of the aircraft:

- A morphing Droop Nose that substitutes the conventional flaps that has better aeroacoustics performances due to a continuous solution that improves both the take-off and landing operation and cruise condition performances [2][3][4][5][6][7]
- A morphing flap, used in combination with the Droop Nose for the high-lift conditions and standalone in cruise condition[8]
- A morphing winglet with two finger like control surfaces that improves the aerodynamic

performances and can be used to perform maneuver load alleviation [9]

- An Innovative Wing Tip device, equipped with a movable control surface that is used to actively control the dynamic loads (MLA/GLA). [10][11] [12][13]

The program aimed to increase the Technology Readiness Level (TLR) of the devices, reaching a level of detail close to the industrial production (TLR≥6). The winglet and the wing tip will be flight tested by the end of the project, while the droop nose and the flap prototypes underwent functionality tests.

The IWT concept is illustrated in Figure 2: it is an extension of the wing in its plane, more tapered and equipped with a control surface. It is conceived as an extra control surface to be used only for load alleviation and control. In the following the complete design and testing process is presented.

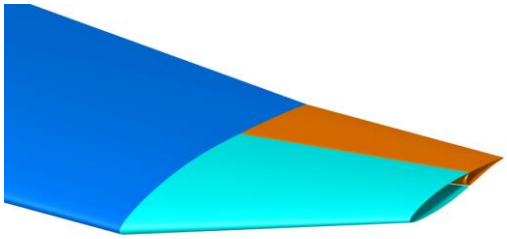

Figure 2 - The IWT concept

2. IWT Development plan

The IET development plan can be divided in four main steps:

1. The identification of the most promising configuration of the IWT, for this reason an extended parametric study identified the better solution for the load alleviation capabilities.
2. The concurrent detailed design of the IWT for all the disciplines involved, like aero-servo-elasticity for the development of the active control laws, the actuation system for the motion of the movable control surface, the structural design to withstands the loads, the aerodynamics to assess the performance improvement achieved with the span extension.
3. The experimental validation of the concept through scaled model to assess and correlate the numerical results. In particular, the ground demo test was propaedeutic to the installation of the item on the aircraft and to achieve the permit to flight for the operative test campaign.
4. Finally, a flight test (2022/2023) will assess the effectiveness of the IWT in an operational environment where the load alleviation capabilities of the IWT will be tested

A schematic representation of the IWT's development is shown in Figure 3

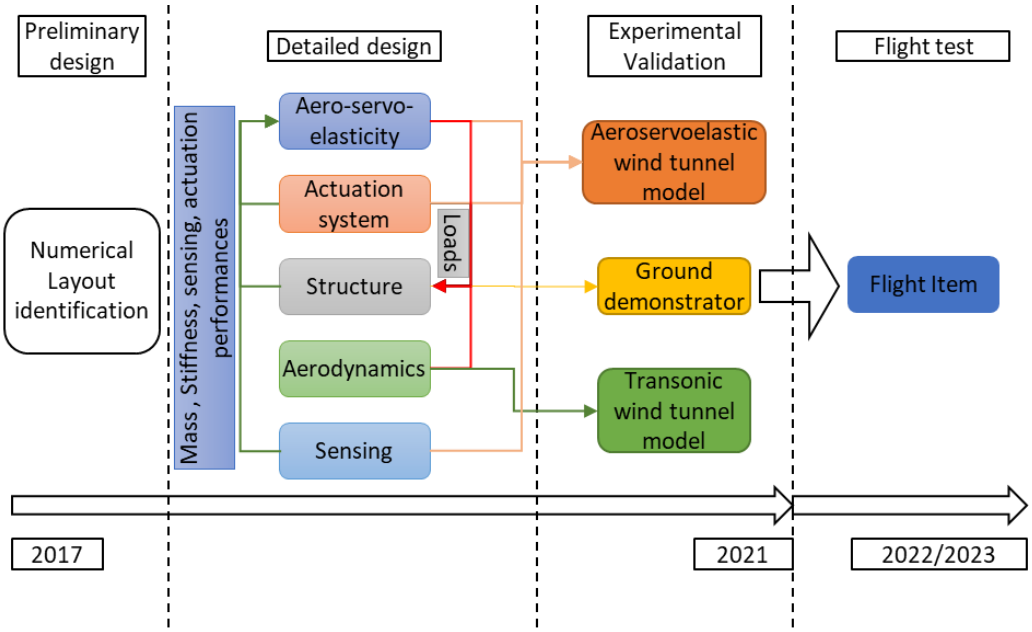

Figure 3 - Development plan of the IWT

The following sections will describe in a deep and extended way the activities performed in the detailed design phase and the experimental validation; the preliminary design phase will be shortly recalled.

3. Preliminary design

In this phase, the concept of the IWT is developed in term of its geometrical configuration, depicted in Figure 4. Starting from the baseline aircraft stick model (FEM + DLM/VLM aerodynamics) a parametric study on the geometrical parameter was performed, identifying the configuration that achieves the better performances from the active load reduction point of view. The full study can be found in [10][11], a summary table of the identified shape is Table 1.

C1/Ctip	C2/C1	e/C1	Sweep	Dihedral	Span
1	0,5	0,35	35°	0°	1m

Table 1 - IWT optimized parameters

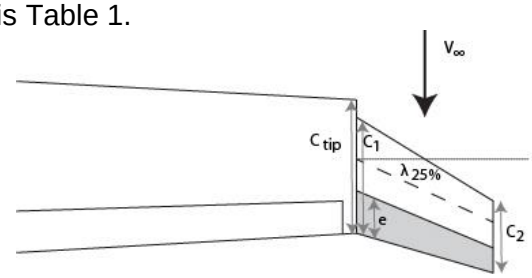

Figure 4 - Geometrical parameters for IWT definition

The stick model, equipped with the identified IWT layout, was used to develop the active control laws as described in [13], whose aim to reduce the gust loads magnitude. The stick model was used to compute the load envelope which provided the sizing loads for the structure and the actuation system.

The output of this phase is the layout of the IWT, which was further developed and designed in all its aspects in the next design phases.

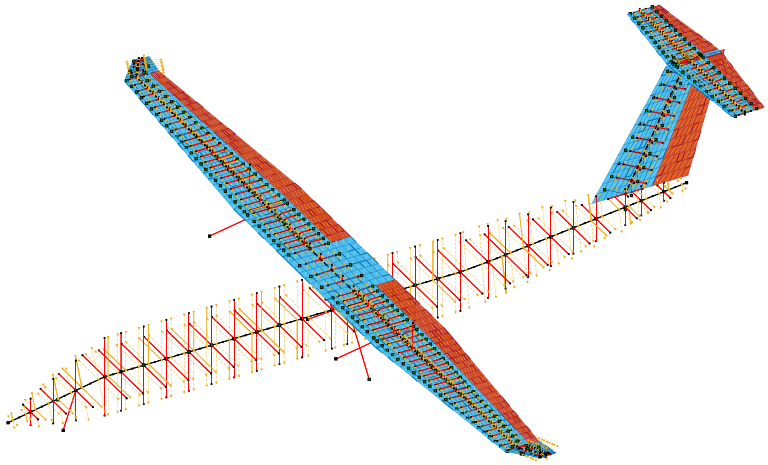

Figure 5 - TP90 aeroelastic stick model

4. Detailed design

This section covers the concurrent detailed design of the IWT for all the disciplines involved and it is divided in three subsections: The first section describes the design and numerical validation of the active control laws for the GLA, in section 4.2 it is presented the design of the actuation system together with the sensors layout, while section 4.3 is about the structural design and analysis of the IWT. It must be pointed out that the sections' numbering does not represent the time evolution of the project, since the design was done concurrently and the modification in one domain was updated in the other disciplines, e.g. modification to the actuation system were translated into the aircraft numerical simulator to evaluate how the performances of the controller were affected.

4.1 Aero-servo-elastic design

The main goal of the IWT is its usage in standalone configuration or in combination with other control surfaces to reduce the gust loads. To do that, dedicated control laws had to be developed to provide the desired deflection of the control surface.

For this reason, the aeroelastic model had to be transformed into a formulation suitable to design and analyze in a fast and robust way the active control laws. The FEM+DLM model was translated into a State-Space (SS) model with the methodology described in [14]. This formulation was employed to

design a Static Output Feedback (SOF) controller [13] using conventional (ailerons and elevator) and non-conventional (IWT) control surfaces to reduce the dynamic loads due to the maneuver and gust. The feedback is based on accelerometers (wing tips and CoG) and Inertial Measurement Unit (IMU) data. The design of the controller was done considering a continuous LTI model where the actuators and the sensors were reproduced with known transfer functions (TF).

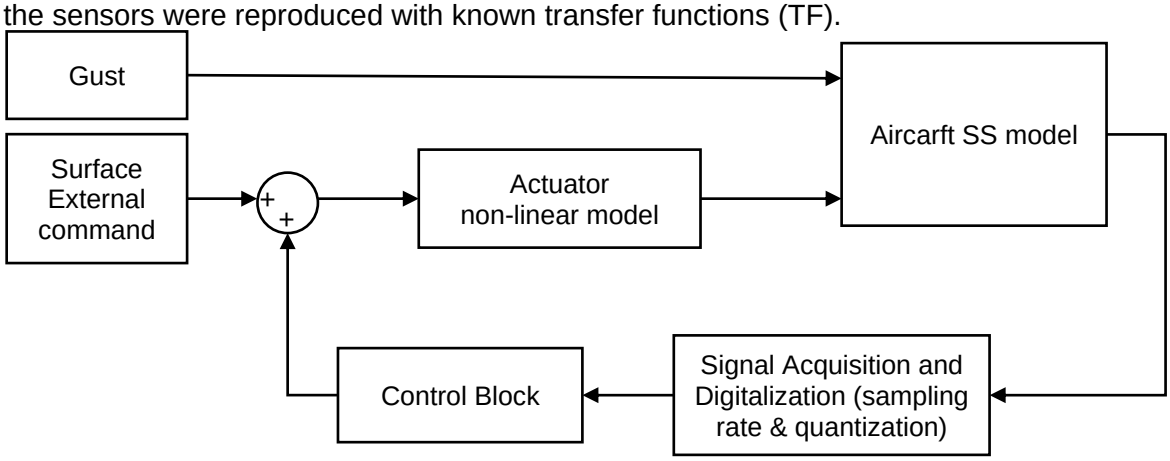

Figure 6 - Block diagram of the Simulink aero-servo-elastic simulator

The output of this activity is an assessment on the effectiveness of the controller and the actuation performances required (hinge moments and actuator bandwidth), used to define the actuation layout.

When the actuation and sensing configurations were frozen, the Simulink model of complete aircraft was digitalized substituting the actuators TF with their equivalent Simulink block that included saturations (position, rates and torques). The sampling times of the measures were uniformed to the one available on the aircraft selected for in flight validation and the controller frequency was set equal to the Flight Control Computer one.

It is clear how the project had to evolve concurrently and how each disciplinary models had to be updated with the output of other intermediate steps.

4.2 Actuation and sensing

The information gathered in the previous section were the inputs to design the actuation system, the hinge moment /rotation (Figure 7) and hinge moment/ angular speed (Figure 8) of the IWT control surface were used to establish the stroke/force and bandwidth characteristics of the actuator to be used. This part was in charge of Umbra Group, a project's partner that is a manufacturer of Electro Mechanic Actuators (EMA).

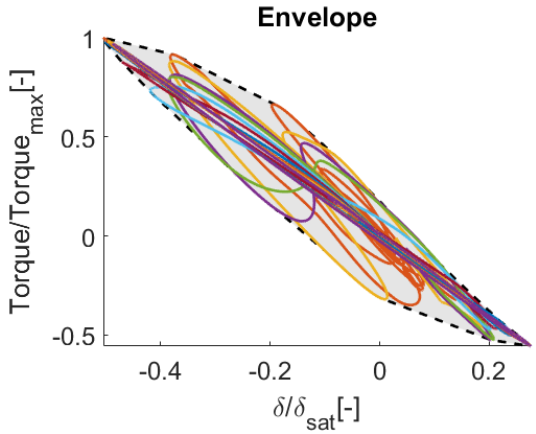

Figure 7 - Torque Vs. Rotation

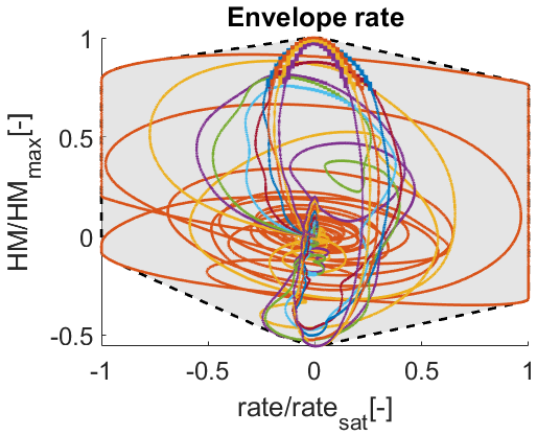

Figure 8 - Torque Vs. Rotation rate

The enveloping conditions were used to design an actuation system (EMA + kinematic chain) that ensured the required performances. The EMA is depicted in Figure 9: it is placed inside the wingbox of IWT and is connected to the movable and fixed part with a screwed joint on the two ends uniballs.

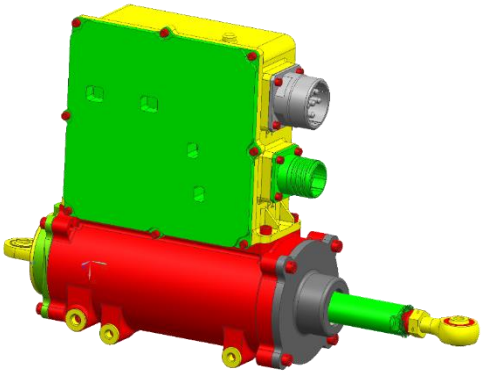

Figure 9 - EMA CAD, courtesy of UMBRA

The pins positions (fixed and movable part) were optimized to fit the physical actuator inside the wingbox and to minimize the actuation force. Figure 10 shows the kinematic of the actuation system and its characteristic measures.

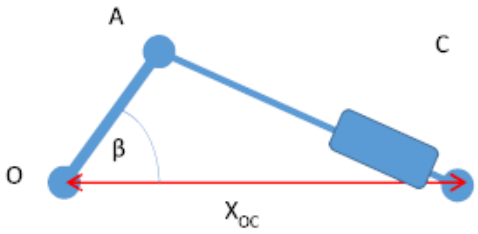

Crank [OA]	**105**	**mm**
Pin to pin [AC] @ zero position	288	mm
Beta @ zero position	30	°
Rotation around zero position	±15	°
Total Operating stroke	34,74	mm
Negative stroke	-13,88	mm
Positive stroke	-20,86	mm

Figure 10 - Optimized kinematic

Once frozen the layout and the actuator performances, the equivalent non-linear Simulink model was integrated in the aero-servo-elastic simulator. In this way it was possible to assess the alleviation capability of the GLA controller considering a detailed non-linear dynamic model for the actuation system.

4.3 Structure

The reference TP90 aircraft is a virtual model, used to assess the potential capabilities of the MLA/GLA systems designed. However, to perform a functionality test of the IWT in a relevant environment, such as a flight test, as requested by CS2 program, a retrofitting of the concept on the existing C27J Spartan was done.

The IWT root airfoil was modified to fit the C27J tip section by keeping the same sizes for the movable part. The structural layout of the IWT is inherited by the C27J wingbox layout, hence the three spars concept is extended to the IWT device. The spars are connected to the skin through L-shaped spar caps, and between each caps an additional stiffener is placed. An intermediate rib is placed to stiffen the structure and to distribute the load coming from the actuator. The CAD model of the IWT is illustrated in Figure 11.

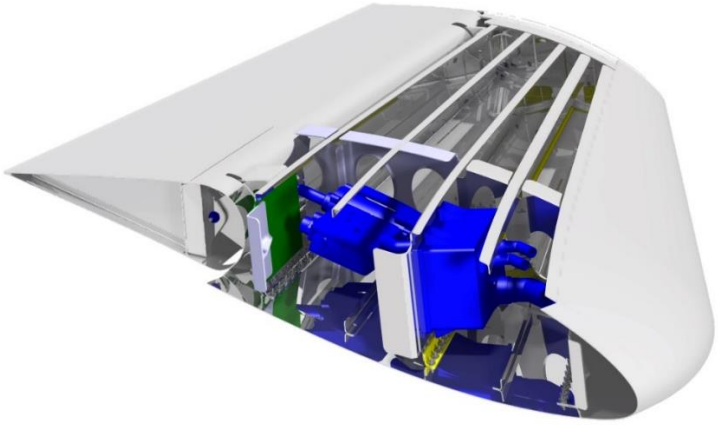

Figure 11 - DMU model of the IWT

The CAD model was then translated into a detailed FEM model, to numerically assess the structural integrity of the IWT and to simulate the static ground test.

Several analyses were performed like static analyses and linear buckling.

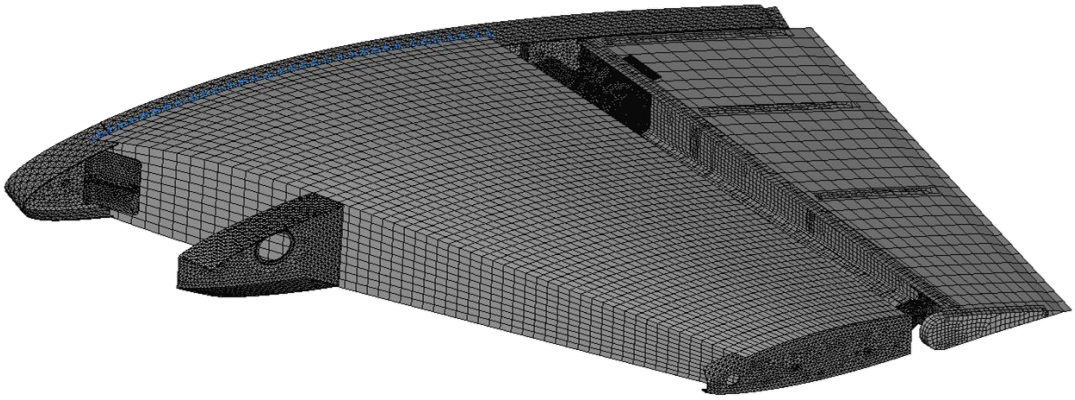

Figure 12 - FEM model of the IWT

Leonardo as the owner of the C27J platform, provided a set of load conditions to be verified and it consisted in 14 load cases (Figure 13). Each load case was provided in term of spanwise distribution of internal forces. The numerical simulation was performed applying the loads in the same points used to load the physical demonstrator (Section 5.3), hence approximating the internal forces distribution.

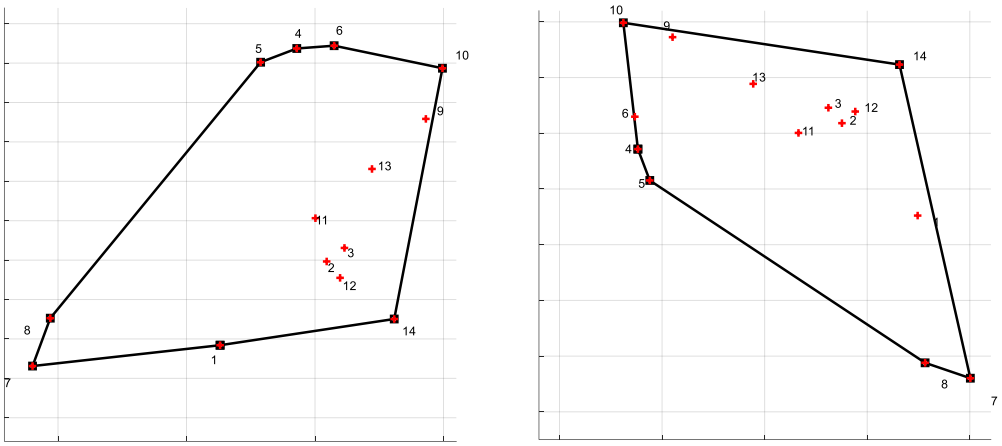

Figure 13 - Torque-bending (left) and shear-torque (right) envelopes at the IWT root

The loading methodology is represented in Figure 14: two load points were selected in correspondence of the two ribs (stiff points), hence the arms with respect to the IWT root are known and they are 0.372m and 1m. Through the arms it is possible to find the value of **F1** and **F2** applied forces to match the bending moment distribution. Given the spanwise position and the magnitude of the loads, their chordwise position (**d1** and **d2**) is computed to approximate the torsional moment distribution.

This led to a total of 14 enveloping load cases applied to the FEM model by mean of rigid elements (RBE3) as in Figure 14.

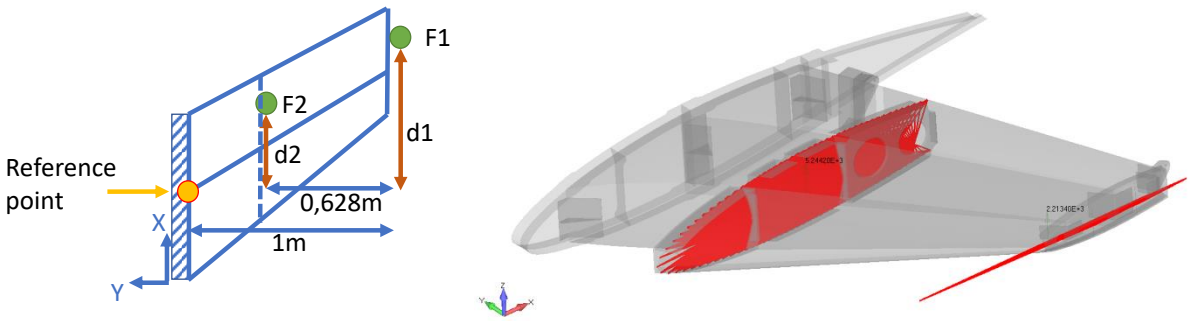

Figure 14 - Loading scheme (left) and position of the rigid elements in the FEM model (right)

Figure 15 shows the internal forces distribution provided (black dashed lines) and the internal forces distribution reproduced with the FEM (continuous lines).

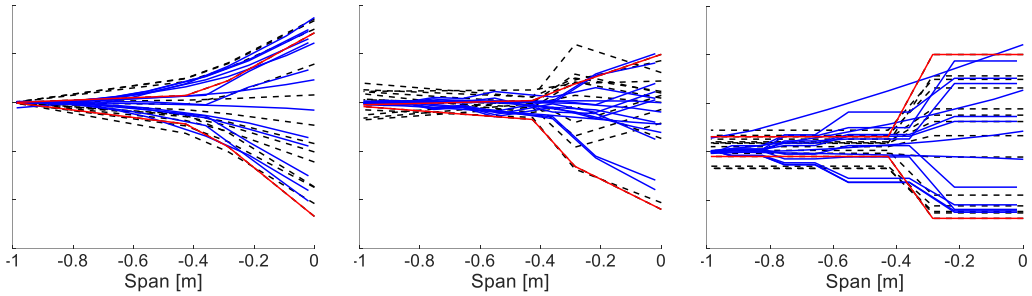

Figure 15 - Bending, Shear and Torque spanwise distribution in the left IWT

The internal forces provided the load to be applied for the fixed part investigation, the movable part must be analyzed as well. In this case the load is provided as distributed external loads, hence it was possible to apply them directly to the structure. Anyway, during the ground demonstrator testing it was possible to load the structure in only two points, for this reason the distributed loads (black arrows in Figure 16) are reduced to two equivalent forces (blue arrows). Figure 16 shows that this approach is conservative (higher internal forces) and then it can be applied to assess the structural integrity of the flap.

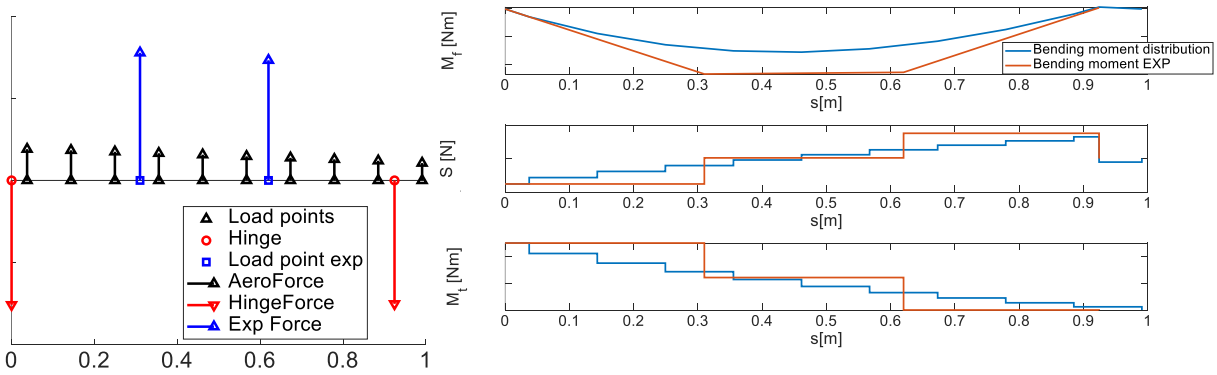

Figure 16 - Aerodynamic distributed forces vs concentrated loads (left) comparison of the obtained internal forces (right)

The load conditions were analyzed with a static linear solver (Nastran SOL101), the results in term of enveloping Von Mises stress, configuration ID and Margin of Safety, are reported in Figure 17 and Figure 18. The Margin of Safety is computed as: $MS = \frac{\sigma_{yielding}}{\sigma_{VM}} - 1$

For all the load cases the minimum MS is around 2, meaning that the loads can be increased 2 times before failure, hence the structure is safe. The same analyses were repeated using ultimate loads (1.5 factor) and evaluating the MS with the ultimate tensile stress, providing results similar to the nominal case.

Figure 18 shows the lowest eigenvalue for linear buckling analysis $\lambda = 5.56$, meaning that the structure won't buckle under the loads.

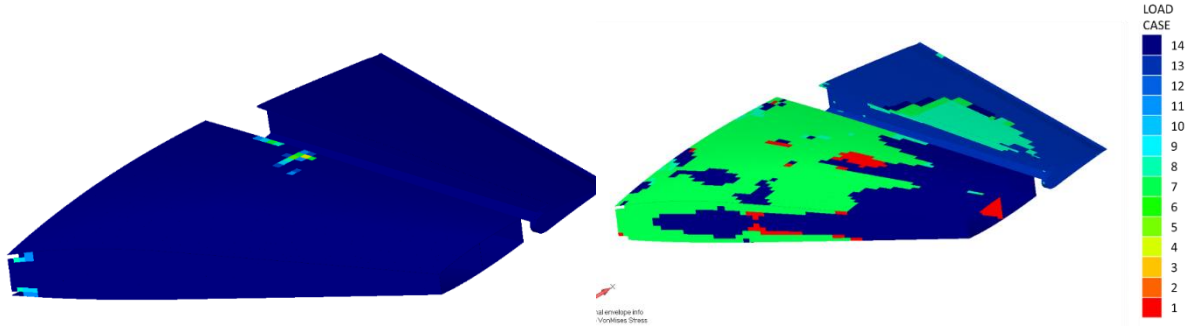

Figure 17 - MoS envelope (left) and most critical condition (right)

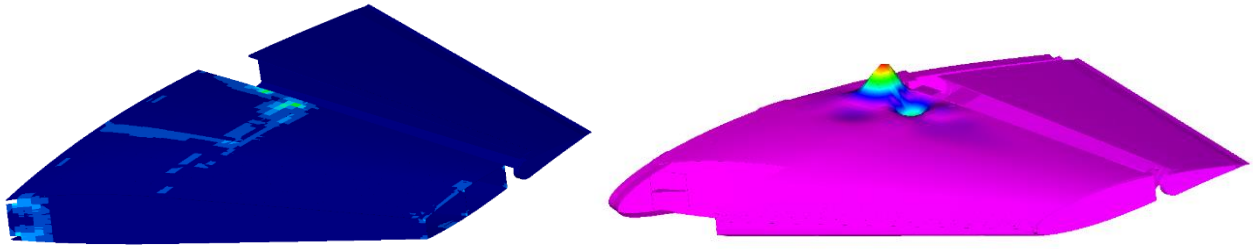

Figure 18 - Von Mises envelope (left) and first buckling mode (right)

Other conditions were simulated, like the loading of the hinges and of the elements that connects the actuator to the structure. Particular attention was paid to the actuator runaway, where the control surfaces is pushed against the end-stop.

The final aspect that had to be verified was the integrity of the connections among the structural element, realized with rivets. The connections were evaluated with an analytical method, the ultimate load for each rivets line was obtained starting from the shear flow q in the element around the connection and considering a safety factor of 1.5, a fitting factor of 1.15 and the rivet spacing. No critical elements have been identified.

5. Experimental validation

Many disciplines were involved in the design of the IWT and before flight test a set of experimental tests at different scale were performed to prove the effectiveness of the item (wind tunnel tests) and to verify the structural integrity of the item under the most severe load conditions. Three experiments were realized and in the following described.

5.1 WTT3, aero-servo-elastic wind tunnel model

This 1:6 scaled half-model, described in [12] and in [13] is an aero-servo-elastic test bench of the real aircraft, thanks to the iso-frequency scaling methodology adopted and the gust generation system of the wind tunnel it was possible to test the Gust Load Alleviation (GLA) controllers in a safe and controlled environment to assess the numerically predicted alleviation.

In this process, the effectiveness of the IWT as a device for GLA/MLA purpose was assessed.

In fact, the model is equipped with movable control surfaces actuated by servomotors that can reproduce the dynamic characteristics of the real actuators in term of bandwidth, rotation, and rotation rate saturation.

The experimental set up is shown in Figure 19, where the half model of the TP90 aircraft is vertically mounted in the wind tunnel and two of the six vanes used for the gust generation can be seen in the background. The model is connected to a pivot-sledge mechanism that reproduce the pitch and plunge free body motion, the sledge is actuated with an electrodynamic actuator (Weight Augmentation System) that allows to produce the weight force and trim the aircraft, performing a trimmed gust simulation.

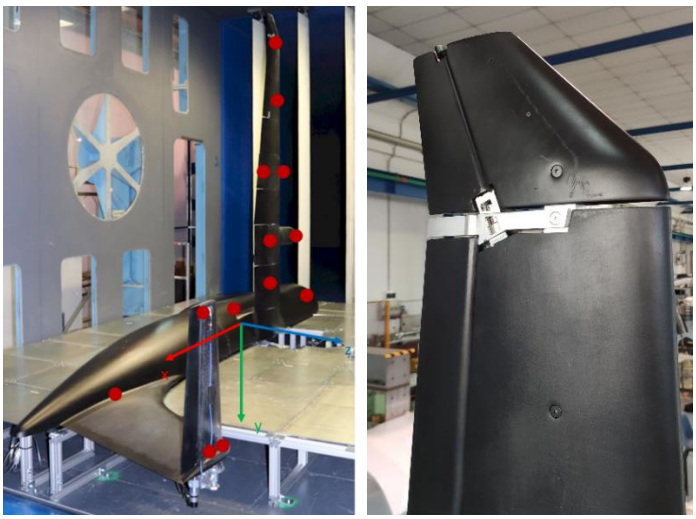

Figure 19 - WTT3 in the wind tunnel test room, markers identify the accelerometers' location (left), IWT mounted on the

wing tip (right)

The feedback for the controller is provided by the acceleration measured at the wing tip and on the CG by two accelerometers and the IMU data measured on the CG, which are the same measure available on the aircraft. The sampling and controller frequency were set to match the hardware installed on the reference aircraft.

The tests were performed considering two (scaled) flight points and two different gusts, one tuned on the 1st bending mode frequency and the other equivalent to the one which produces the highest Wing Root Bending Moment (WRBM), both with positive and negative amplitude, for a total of 8 gust conditions. Figure 20 compares the numerical and experimental results obtained for two different controllers: the SOF003 used the IWT only to perform the GLA, and the SOF401 which used all the available control surfaces (IWT, aileron and elevator). The SOF003 controller has a mean alleviation around 5%, while all surfaces controller reaches 20% mean alleviation. These two cases show how the IWT can be used as a standalone control surface or in combination with the primary control surfaces to alleviate the gust loads. For both the controllers the experimental results are aligned with the numerical ones, while some differences are due to the experimental set-up that did not reproduce completely the free body motion (friction issues), for this reason the feedback from the rigid body state is limited and hence the control deflection required by the control law.

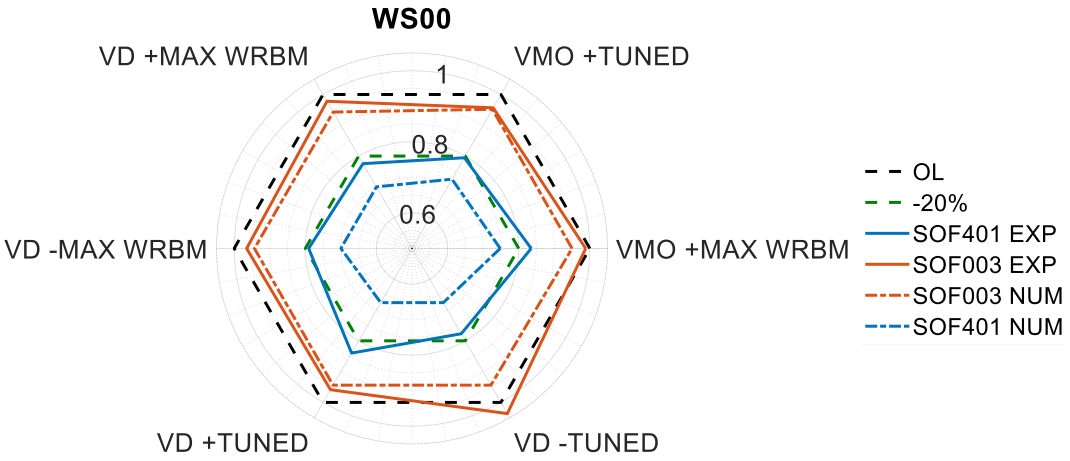

Figure 20 - Comparison of different controllers' effectiveness, numerical vs wind tunnel results

The wind tunnel test proved the effectiveness of the IWT as an active control device, obtaining results fully comparable with the numerical ones. Better performance in term of alleviation can be achieved when the IWT is used in combination with conventional control surfaces.

5.2 WTT2, high speed and high Mach wind tunnel model

This WTT2 wind tunnel model is a 1:3 scaled model of the TP90 wing only. It was designed to assess the aerodynamic performance of the wing in its reference condition and with the devices developed in the CS2 research program. The model, equipped with droop nose (DN), a morphing flap (MF), finger-like winglet (WLET) and IWT was tested in high-speed conditions at DNW facility to evaluate the efficiency of the different devices and the static load alleviation capabilities (WLET and IWT of Figure 21).

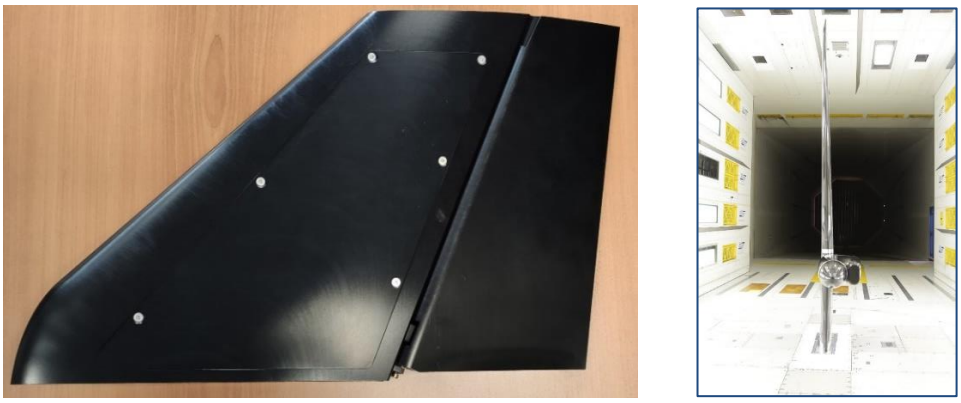

Figure 21 - IWT 1:3 model

5.3 GD, ground demonstrator for static test

The most important test to both validate the IWT design and to achieve the permit to flight o test the IWT in a relevant operative environment is the structural qualification of the item. For this reason, a ground demonstrator of the IWT was realized and was tested applying the nominal loads. Among the 14 sizing conditions, the two worst conditions (ID=7 and ID=10) in term of root bending and torque moment were down selected and reproduced on the ground demonstrator.

A dedicated test rig (Figure 22) was built to accommodate the IWT in vertical position, clamped at its root by an interface rib, the load was produced with two hydraulic actuators and transferred to the fixed structure of IWT by means of two load saddle. Strain (Figure 23) and displacement (Figure 22) measures were collected to perform a comparison with the numerical results and to check the linearity of the strains under a loading/unloading process, hence to detect material yielding or buckling during the test. Moreover, the strain gages are connected to realize a set of Wheatstone's bridges (Figure 23) to measure the internal forces in the IWT (bending, torque and shear) in two spanwise stations. This choice was done in view of flight tests, where it is required to monitor the loads and the ground demo tests provides a first calibration of the IWT.

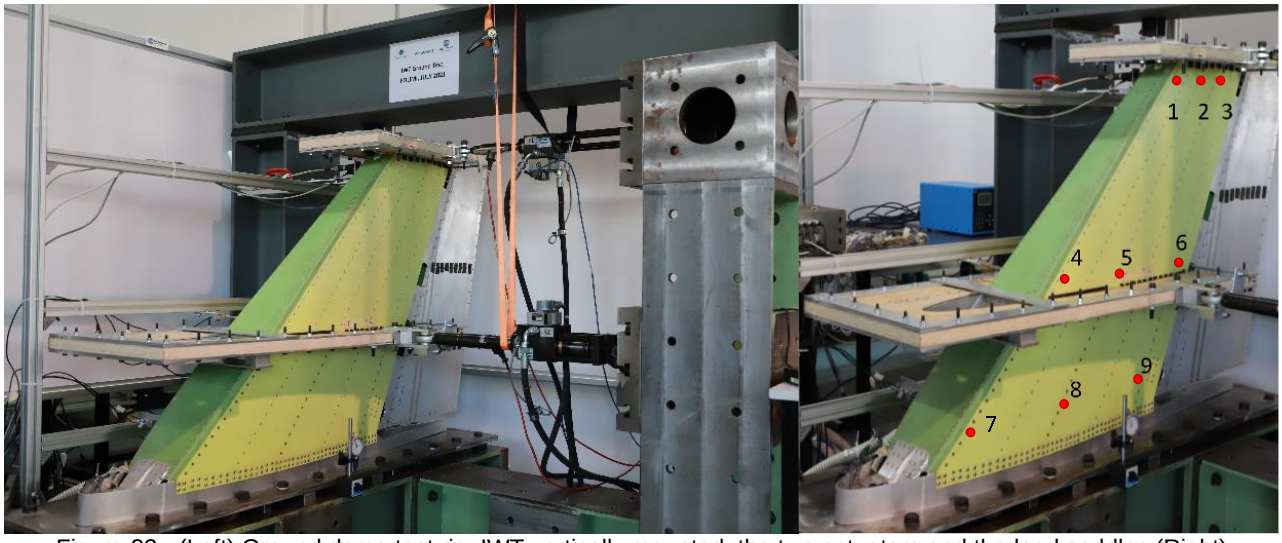

Figure 22 - (Left) Ground demo test rig: IWT vertically mounted, the two actuators and the load saddles (Right) displacement measurement points

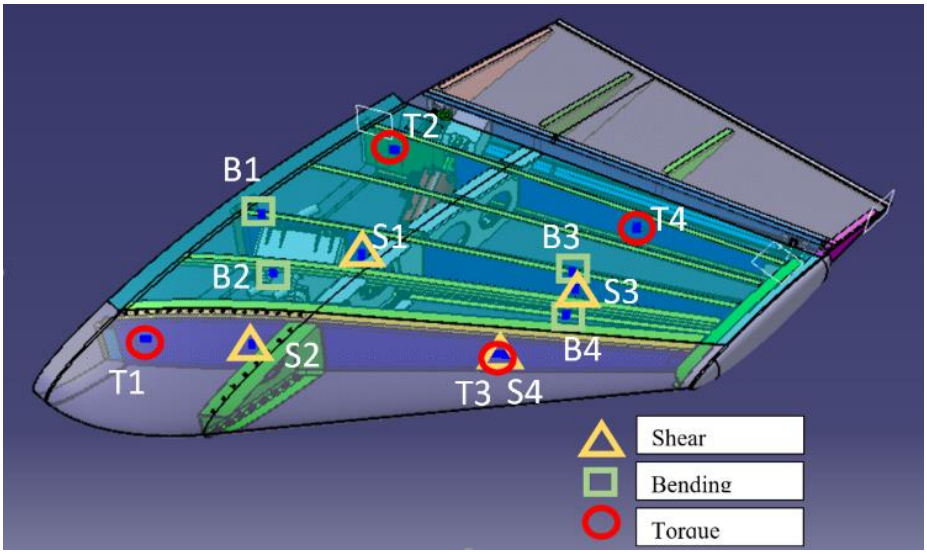

Figure 23 - strain gage layout for bending, shear and torsion measures

The tests were performed with a stepped pyramidal approach: the load was increased and then hold to a fixed value for about 2 minutes so the structure can settle down in the new configuration. The tests were performed multiple times to check eventual backlash in the structure.

As done for the fixed part the IWT, the structural tests were performed on the flap. The control surface was hold in a fixed position by a rod which substituted the actuator, and the load was applied with a mechanism similar to the one used for the fixed part. In this case a single actuator was employed, and the load transferred to the structure through a load tree, resulting in two concentrated forces. Beyond the structural integrity of the component, this test was crucial to tune the strain gauge installation (Figure 24 left) able to measure the hinge moment during the flight. Figure 24 right shows the relation between the applied moment and strain measured obtained with a half-bridge for torsion on the upper and on the lower skin of the flap. The behavior is linear, and a calibration process can be used to obtain the measure of the hinge moment during flight tests.

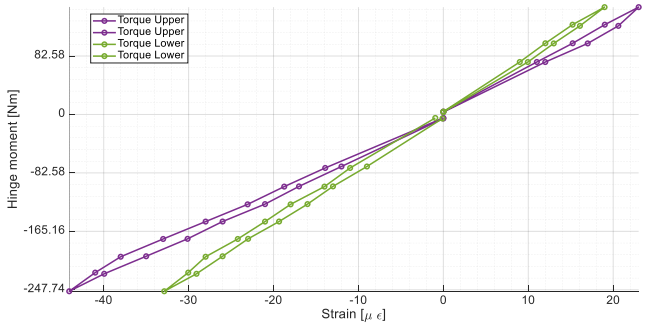

Figure 24 - Strain gauge on the flap skin (left) and hinge moment versus strains, downward and upward rotation together (right).

The IWT was tested until Limit Loads as requested, showing a linear behavior without any kind of local failure or permanent deformation.

6. Road to flight tests

In May 2022 it was ended the manufacturing of the flying IWTs and their functionality was assessed by TECNAM. In the next months the items will be delivered to Leonardo and mounted on an instrumented C27J aircraft for the flight test, which will be performed in quiet air and in a limited flight envelope. During this test, a set of maneuvers will be performed to assess the load alleviation capabilities of the IWT in an operational environment.

Figure 25 - Final assembly of the left and right IWTs which will be installed on the flying testbed, courtesy of TECNAM

7. Conclusion

This work illustrated the development of an innovative wing tip device to actively alleviate the dynamic and maneuver loads. The process involved several disciplines with different levels of detail, remarking the multidisciplinary of the aircraft design, even when only a component (IWT) is designed. The process covered all the aspects of the design, from the conceptual level to the installation on a real aircraft. Intermediate experiments were employed to assess the performances of the item for different disciplines, increasing the TLR of the device.

8. Acknowledgements

The research described in this document has been carried out in the framework of AIRGREEN2 Project, which gratefully received funding from the Clean Sky 2 Joint Undertaking, under the European's Union Horizon 2020 research and innovation Program, Grant Agreement No. 807089-REG. A special thanks to Prof. Paolo Mantegazza for his continuous support.

9. Contact Author Email Address

Mailto: Francesco.toffol@polimi.it

10. Copyright Statement

The authors confirm that they, and/or their company or organization, hold copyright on all of the original material included in this paper. The authors also confirm that they have obtained permission, from the copyright holder of any third-party material included in this paper, to publish it as part of their paper. The authors confirm that they give permission or have obtained permission from the copyright holder of this paper, for the publication and distribution of this paper as part of the ICAS proceedings or as individual off-prints from the proceedings.

References

[1] Ameduri, S. et al. "An Overview of the AG2 Project: Latest Achievements", in: AIAA Scitech 2022 Forum. 2022. p. 0717.

[2] Ricci, S., De Gaspari, A., Gilardelli, A., Airoldi, A., "Design of a leading edge morphing based on compliant structures for a twin-prop regional aircraft", AIAA/AHS adaptive structures conference,1063, 2018.

[3] De Gaspari, A.,"Multiobjective Optimization for the Aero-Structural Design of Adaptive Compliant Wing Devices", Applied Sciences,10,18,6380, 2020, Multidisciplinary Digital Publishing Institute.

[4] De Gaspari, A., Gilardelli, A., Ricci, S., Airoldi, A., Moens, F., "Design of a leading edge morphing based on compliant structures in the framework of the CS2-AirGreen2 project", "Smart Materials, Adaptive Structures and Intelligent Systems", 51944, V001T04A025, 2018, American Society of Mechanical Engineers-

[5] De Gaspari, A., Moens, F.,"Aerodynamic Shape Design and Validation of an Advanced High-Lift Device for a Regional Aircraft with Morphing Droop Nose", *International Journal of Aerospace Engineering*, vol. 2019, Article ID 7982168, 21 pages, 2019. https://doi.org/10.1155/2019/7982168

[6] De Gaspari, A., Cavalieri, V., Ricci, S., "Advanced Design of a Full-Scale Active Morphing Droop Nose", *International Journal of Aerospace Engineering*, vol. 2020, Article ID 1086518, 19 pages, 2020.

https://doi.org/10.1155/2020/1086518.

[7] Cavalieri, V. De Gaspari, A. and Ricci, S., "Optimization of compliant adaptive structures in the design of a morphing droop nose", *Smart Materials and Structures*, 29, 7, 075020, 2020, IOP Publishing.

[8] Pecora, R., "Integrated design approaches for an innovative multifunctional flap architecture based on distributed electromechanical actuation", AIAA Scitech2022 Forum,0719, 2022.

[9] Dimino, I., Moens, F., Pecora, R., De Gaspari, A., Ricci, S., Ameduri, S., Concilio, A., Mercurio, U., Carossa, G., "Morphing Wing Technologies within the Airgreen 2 Project", AIAA Scitech 2022 Forum, 0718,2022.

[10] Fonte, F., Toffol, F., Ricci, S., "Design of a wing tip device for active maneuver and gust load alleviation". AIAA/ASCE/AHS/ASC Structures, Structural Dynamics, and Materials Conference. 2018. p. 1442.

[11] Toffol, F., Fonte, F., Ricci, S.," Design of an innovative wing tip device", 17th International Forum on Aeroelasticity and Structural Dynamics (IFASD 2017). 2017. p. 1-16.

[12] Ricci, S., et al., "Design and Experimental Validation of Gust Load Alleviation Systems based on Static Output Feedback", AIAA Scitech 2022 Forum. 2022. p. 0441.

[13] Toffol, F., et al., "Gust and Maneuver Loads Alleviation Technologies: Overview, Results and Lesson Learned in the Framework of the CS2 AIRGREEN2 project". 19th International Forum on Aeroelasticity and Structural Dynamics (IFASD 2022), Madrid.

[14] Ripepi, M., and Mantegazza. "Improved matrix fraction approximation of aerodynamic transfer matrices.", *AIAA Journal* 51.5 (2013): 1156-1173.